

Fouling behavior and scaling mitigation strategy of CaSO₄ in submerged vacuum membrane distillation



Tong Zou^{a,b}, Xiangling Dong^{a,b}, Guodong Kang^{a,*}, Meiqing Zhou^a, Meng Li^a, Yiming Cao^{a,*}

^a Dalian National Laboratory for Clean Energy (DNL), Dalian Institute of Chemical Physics, Chinese Academy of Sciences, Dalian 116023, China

^b University of Chinese Academy of Sciences, Beijing 100049, China

ARTICLE INFO

Keywords:

Submerged membrane distillation
Fouling
Scaling mitigation
Air backwash

ABSTRACT

Fouling and scaling in membrane distillation (MD) is one of the major obstacles to its long term stability. Submerging the membrane directly into the feed is an alternative method to prevent flow channel blockage. The fouling behavior of CaSO₄ in submerged vacuum membrane distillation at varying experimental conditions was investigated. It presented a two-stage trend when the initial concentration of CaSO₄ was < 2700 mg/L. Dramatic flux decline occurred once the feed was concentrated to a critical level of saturation. A on-line periodically air backwash was applied to reduce CaSO₄ crystals deposition on the membrane surface or penetration in the membrane pores. While the role of air bubbles in affecting the fouling behavior of CaSO₄ largely depended on the crystal formation mechanism. The fouling rate was reduced by 54% with the help of air backwash when surface crystallization controlled the process while negligible effect was made when bulk crystallization played a more important role. The result could be explained by combining the experimental data with a first-order kinetic model proposed by Tansel. The off-line water cleaning suggested that the fouling layer could be removed effectively without additional chemical agent.

1. Introduction

Membrane distillation (MD) is a thermally driven technology using porous hydrophobic membrane as an unselective barrier to achieve distilled water production or aqueous solution concentration [1]. The nonvolatile components in feed solution can be rejected on one side of membrane while the vapor molecules are transported to the other side due to the vapor pressure difference. Besides the general advantages such as lower operating temperature than conventional distillation, lower operating hydrostatic pressure than pressure-driven processes and higher rejection factor of non-volatile solutes, the most prominent potential of MD technology lies in its unique ability to treat high salinity solutions [2,3]. Since water flux is not influenced by the osmotic pressure gradient, the process of MD can maintain relative sustainability without suffering from large permeate loss for the highly concentrated solution which is close to or even higher than the saturation point [4,5].

Despite the fact that MD has been increasingly studied over the last few years, membrane fouling, caused by accumulation of undesired materials on the membrane surface or in the membrane pores, is still an urgent issue which affects the long term stability of MD like all other membrane processes [1,6]. The existence of fouling layer not only adds

additional heat and mass transfer resistances, but also increases the risk of pore blockage and membrane wetting, and finally results in deterioration of MD performance [7]. Therefore, it is necessary to understand the fouling behavior and find out effective fouling control techniques for specific pollutants. The types of pollutants existed in MD process can be mainly classified into inorganic pollutants, particulate pollutants and biological pollutants [8]. As most of the reverse osmosis retentate contains large amount of scaling ions, the research of inorganic fouling caused by sparingly soluble salts is of most concerned in literature [9,10].

Fouling in MD process is a complicated phenomenon which is significantly influenced by many factors, and the configuration of membrane module is one of them. It is worth noting that most of MD studies use conventional cross-flow hollow fiber module, which has strong inclination to fouling and is difficult for cleaning and maintenance [11]. This problem can potentially be minimized by submerging the membrane into the feed directly [12,13]. Fouling control techniques can influence fouling behavior as well, different strategies such as feed pretreatment [14,15], membrane surface modification [16,17] and chemical cleaning [18] have been studied to alleviate or eliminate the negative effect of fouling in varying degree. Bubble-assistant technology is considered as an effective way to remove deposition layer

* Corresponding authors.

E-mail addresses: kanguod@dicp.ac.cn (G. Kang), ymcao@dicp.ac.cn (Y. Cao).

from membrane surface especially for submerged membrane filtration process [19,20]. Recently, this method is gradually applied to MD process. Chen et al. reported that the scaling formation in direct contact membrane distillation could be alleviated by introducing gas bubbles when treating NaCl solution [21]. Ding et al. also found that intermittent gas bubbling reduced membrane fouling in concentrating traditional Chinese medicine [22]. However, opposite conclusion was made by Meng et al., i.e., bubbles generated through air backwash increased salt deposition when feed solution contained sparingly soluble salts [13]. Therefore, further investigation is still needed to find out the role of air bubbles played in membrane fouling for specific pollutants.

In this paper, a self-made open membrane module was designed using polytetrafluoroethylene (PTFE) hollow fiber membranes. The submerged vacuum membrane distillation (SVMD) was used to reduce the risk of feed flow blockage and make it convenient for module cleaning. The main objective of this study was to investigate the effect of two different crystal formation mechanisms on the fouling behavior of CaSO₄ and the role of air backwash played in scaling mitigation in both cases. In addition, an empirical flux decline model was used to further explain the experiment results.

2. Experimental

2.1. Materials and membrane module

PTFE is a good candidate for MD due to its superior hydrophobicity, thermal stability, chemical resistance and mechanical strength [23,24]. Self-made microporous PTFE hollow fiber membranes [25] were used and sealed with an epoxy resin at both ends to fabricate a simplified open membrane module in this study. The characteristics of hydrophobic membranes and membrane module are listed in Table 1.

2.2. Feed solution

Calcium chloride and sodium sulfate were purchased from Tianjin Kemiou Chemical Reagent Company and used without further purification. The feed solution was prepared by mixing appropriate amount of fully dissolved CaCl₂ and Na₂SO₄ with deionized (DI) water as solvent.

Prior to all experiments, DI water was used as feed solution for 1 h to get initial pure water flux J₀.

2.3. Experimental design

The SVMD system was used in this study (Fig. 1). A curtain type of hollow fiber membrane module was simply submerged in a constant temperature feed tank, in which the outer surface of the hollow fiber membranes was contacted with hot feed solution directly. The volume of the initial feed solution was always 16 L. The feed temperature in this

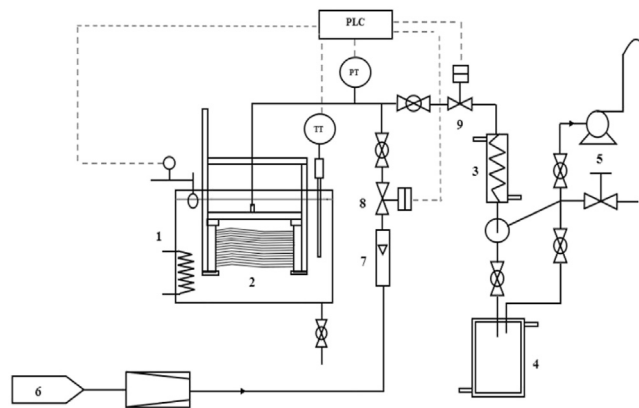


Fig. 1. Schematic of the SVMD setup. 1. Constant temperature feed tank. 2. Curtain type hollow fiber membrane module. 3. Condenser. 4. Permeate tank. 5. Circulating water vacuum pump. 6. Air compressor. 7. Air flow meter. 8. Intake valve. 9. Vacuum valve.

study was in the range of 70–80 °C and was controlled by a Pt-100 temperature sensor with accuracy of ± 0.5 °C. Vacuum pressure of the permeate was maintained at – 85 KPa (± 1.0 KPa) controlled by a vacuum valve. Both Pt-100 temperature sensor and vacuum pressure were connected to PLC system.

Permeate was collected in the permeate tank and its weight was measured by an electronic balance. Permeate flux was calculated using the equation as follows:

$$J \left[\frac{\text{kg}}{\text{m}^2 \cdot \text{h}} \right] = \frac{m}{A \cdot t} \tag{1}$$

where, *m* is the weight of permeate (kg), *A* is the effective area of membranes (m²) and *t* is the operation time (h).

Permeate conductivity was continuously monitored by a conductivity meter. Salt rejection was calculated using the following equation:

$$R [\%] = \frac{C_f - C_p}{C_f} \times 100 \tag{2}$$

where, *C_f* and *C_p* is the conductivity of the feed and permeate, respectively.

The flux data were presented in terms of normalized flux ratio *J*/*J*₀ [26]. Where *J* is the instantaneous flux and *J*₀ is the initial flux when

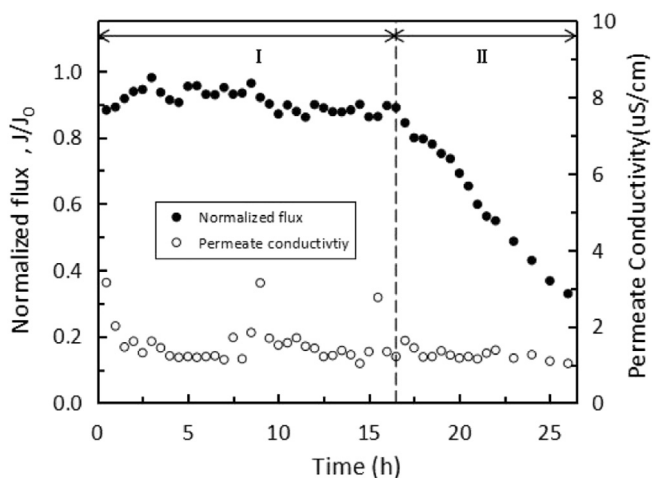


Fig. 2. Normalized flux ratio and permeate conductivity as a function of operation time for concentrating 1800 mg/L CaSO₄ solution. The initial pure water flux was 4.2 kg/m²·h. Experiment conditions: feed temperature 75 °C; vacuum pressure – 85 KPa.

Table 1
The characteristics of the PTFE hollow fiber membranes and membrane module.

PTFE hollow fiber membrane properties	
Outer diameter (mm)	1.693
Inner diameter (mm)	0.862
Wall thickness (mm)	0.415
Porosity (%)	0.411
Mean pore diameter (μm)	0.186
Tortuosity	2.619
LEP _w (bar)	3.2
Membrane module for SVMD	
Effective length of membranes (cm)	23.2
No. of PTFE hollow fibers	55
Effective area of membranes (m ²)	0.068

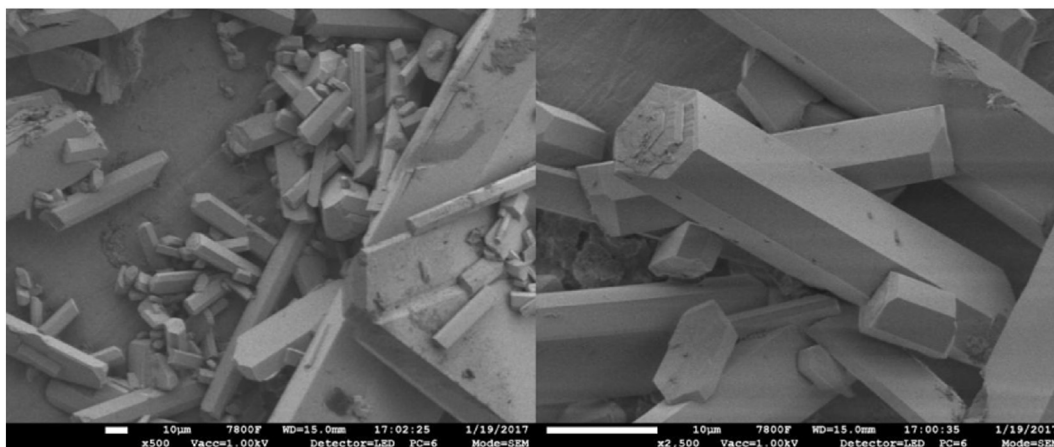


Fig. 3. SEM micrographs of the CaSO₄ fouling layer after experiment. The magnifications were 500 times for the left and 2500 times for the right.

using DI water as feed solution. The rate of change of the flux reduction can be used to reflect the rate of membrane fouling. The fouling rate was calculated using the Eq. (3) [8].

$$\text{Fouling rate} \left[\frac{\%}{\text{h}} \right] = \frac{\text{Flux}_{\text{initial}} - \text{Flux}_{\text{final}}}{\text{Flux}_{\text{initial}}} \times \frac{100}{t} \quad (3)$$

The concentration factor was the ratio of the concentration in the concentrate to that in the initial feed solution.

At the completion of each experiment, the membrane module was taken out from the feed tank and immersed in the DI water for several hours to remove the fouling layer. Pure water flux was retested and the membrane module was continued to use if the flux recovery was > 95%.

2.4. Surface characterization techniques

The morphology of the fouling layer deposited on membrane surface was examined by a JSM-7800F Scanning Electron Microscope (SEM). The membrane samples were dried in a natural environment and coated with gold in a vacuum environment. The fouled membrane samples were taken from the module and cut gently to make sure the deposited fouling layer was not destroyed.

3. Results and discussion

3.1. Fouling behavior of CaSO₄ concentration process in SVM

CaSO₄ was selected as feed solution in this study considering its high scaling tendency compared to CaCO₃ and silicate [10,27]. The 1800 mg/L CaSO₄ feed solution which is closed to saturation point was tested (maximum saturation concentration is about 2000 mg/L at 40 °C). As the saturation concentration increased, the fouling behavior of CaSO₄ presented a two-stage trend with the normalized flux ratio remained almost stable in the first stage and then followed by a

Table 2
Operation time, fouling rate and concentration factor in each stage.

	Stage I	Stage II
Operation time (h)	16.5	9.5
Fouling rate (%/h)	0	6.63
Concentration factor	1.78	2.37

dramatically flux decline in the second stage which was shown in Fig. 2.

In the first stage, crystals formed both on the membrane surface and in the bulk solution were negligible. But membrane surface crystallization occurred once the concentration factor was above a critical level. At the end of the second stage, a dense fouling layer could be observed obviously on the membrane surface with naked eyes. The fouled membrane sample was taken out for further investigation. SEM analysis (Fig. 3) showed that a layer of large cubical shaped CaSO₄ crystals were nonuniformly covered on the membrane surface.

In MD process, the reason of flux decline is attributed to the combination of concentration polarization, membrane fouling and membrane pore wetting [7]. As the permeate conductivity maintained a relatively low level in the range of 1–3 μS/cm throughout the test (Fig. 2), it is believed that the membranes do not suffer pore wetting. With the increase of concentration factor, the concentration polarization was also expected to increase leading to the precipitation of salts on the membrane surface. The main reason for rapidly flux decline in the second stage was the formation and growth of CaSO₄ crystals on the membrane surface. On one hand, the rapid heterogeneous nucleation and growth of CaSO₄ crystals on the membrane surface reduced open pore area available for water to vaporize [28]. On the other hand, precipitation and accumulation of CaSO₄ crystals on the existing nucleation sites additional fouling resistance which was not conducive to the mass and heat transfer in MD process [7].

The corresponding parameters in each stage were summarized in Table 2. The induction time of CaSO₄ under this experimental condition

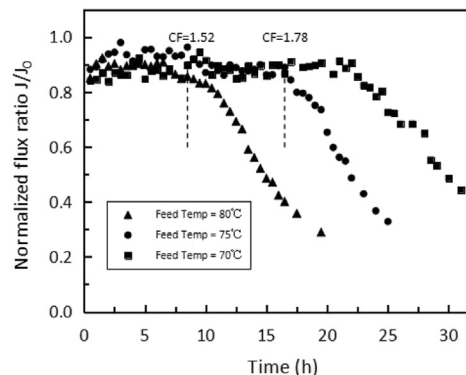


Fig. 4. Normalized flux ratio as a function of operation time at different feed temperatures for concentrating 1800 mg/L CaSO₄ solution. Initial pure water flux for feed temperature of 70 °C, 75 °C and 80 °C was 2.8 kg/m²·h, 4.2 kg/m²·h and 5.3 kg/m²·h, respectively. Experiment conditions: vacuum pressure – 85 KPa.

Table 3

The list of the induction time, critical concentration factor and fouling rate in the second stage for different feed temperatures.

Feed temperature (°C)	70	75	80
Induction time (h)	22	16.5	8.5
Critical concentration factor	1.78	1.78	1.52
Fouling rate in the second stage (%/h)	5.70	6.63	6.02

was 16.5 h and the critical concentration was 1.78. Both the parameters mentioned above show some differences under different operation conditions [10,29], which will be discussed in detail later.

3.1.1. The effect of feed temperature

1800 mg/L CaSO₄ solution was concentrated at 70–80 °C to investigate the fouling behavior of CaSO₄ at different feed temperatures. All curves in Fig. 4 showed a similar two-stage trend as described in Fig. 2. The induction time, critical concentration factor and fouling rate in the second stage at different feed temperatures were listed in Table 3.

It is suggested that the induction time of CaSO₄ crystallization decreased with the increase of feed temperature [30]. The higher the feed temperature was, the greater the collision probability between Ca²⁺ and SO₄²⁻ was, the nucleation rate of CaSO₄ crystallization increased, which resulted in shorter induction period [31]. Once nucleation sites on the membrane surface were formed, CaSO₄ crystals grew rapidly, which was the reason for quickly flux attenuation after critical point appeared.

It is interesting to note that the feed temperature did not have obvious influence on the rate of membrane fouling in the second stage (Table 3). The similar fouling rate demonstrated that feed temperature only affected crystals nucleation rate. Another remarkable point is that the critical concentration factor decreased slightly from 1.78 to 1.52 when the feed temperature increased from 75 °C to 80 °C. The higher temperature on the membrane surface increased the tendency of CaSO₄ crystallization, due to the inverse solubility property of CaSO₄. Therefore, it is not necessary to set the feed temperature too high. As it was shown in Fig. 4, the MD performance seemed more stable at 70 °C with longer induction time, but the critical concentration factors at 70 °C and 75 °C were nearly the same (Table 3), which indicated that the concentration efficiency at 75 °C was higher since higher permeate flux could be obtained at 75 °C. Therefore, the feed temperature of 75 °C is a relatively optimized operation condition for concentrating 1800 mg/L CaSO₄ solution in this study.

3.1.2. The effect of initial feed concentration

The normalized flux ratio as a function of operation time with different initial feed concentrations of 900, 1800, 2700 and 3600 mg/L CaSO₄ solution was investigated. All of the concentration processes were terminated when the normalized flux ratio decreased to approximately 0.3.

CaSO₄ crystallization was a process in which homogeneous nucleation in the bulk solution and heterogeneous nucleation on the membrane surface occurred simultaneously [32]. The different initial concentration of CaSO₄ in feed solution resulted in different fouling behavior directly, which indicated that the dominate crystallization mechanisms were different. As the result showed in Fig. 5, it took a long time prior to the onset of rapid flux decline when 900 mg/L CaSO₄ solution was tested. Increasing the initial concentration of CaSO₄ from 900 mg/L to 2700 mg/L, the induction time was shortened from 34.5 h to only 4 h. With the increase of initial concentration of both Ca²⁺ and SO₄²⁻ in feed solution, both the rate of homogeneous nucleation and heterogeneous nucleation increased to shorten the time of balance between crystallization and dissolution, leading to an earlier occurrence of the critical point. Although the induction time in above three cases

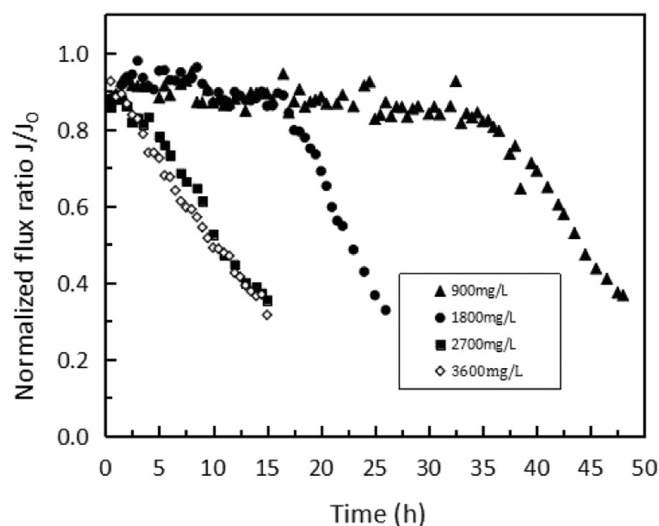


Fig. 5. Normalized flux ratio as a function of operation time with different initial concentration of CaSO₄. Initial pure water flux for initial feed concentration of 900 mg/L, 1800 mg/L, 2700 mg/L and 3600 mg/L was 3.9 kg/m²·h, 4.2 kg/m²·h, 3.8 kg/m²·h and 4.1 kg/m²·h, respectively. Experiment conditions: feed temperature 75 °C; vacuum pressure – 85 kPa.

decreased with the increased of feed concentration, the permeate flux still kept stable for a period of time before rapidly flux decline occurred, which implied that the nucleation and growth of CaSO₄ were gradually development on the membrane surface. It is worth noting that the limited saturation concentration were all above the maximum saturation concentration of CaSO₄, which confirmed that the membrane distillation process can achieve stable operation under a critical level of supersaturation. But when the initial concentration of CaSO₄ increased to 3600 mg/L, a large amount of small CaSO₄ crystals had already precipitated in the bulk solution in the process of heating due to the supersaturated condition of the initial feed. These small CaSO₄ crystals accelerated the homogeneous nucleation in bulk solution and easily migrated to the surface of the membrane to form a deposited fouling layer leading to the disappearance of the induction time and flux decline from the beginning. This different fouling behavior suggested that homogeneous nucleation in the bulk feed may played a dominate role in the fouling process when increased the supersaturation degree of the feed.

In order to illustrated the experiment result, SEM analysis of membrane samples for initial concentration of 900 mg/L and 3600 mg/L were compared (Fig. 6). For 900 mg/L CaSO₄ solution, membrane surface was partially covered with large cubical CaSO₄ crystals and some small nucleation sites could be observed, the fouling layer thickness was thinner. In this case, the main reason for flux decline is the blockage of open pore area caused by crystallization on the membrane surface. While for 3600 mg/L CaSO₄ solution, CaSO₄ crystals were completely covered the membrane surface and the fouling layer became very thick. This additional fouling layer resistance became the main factor of a severe loss of permeate flux.

To further decide the most important factor regarding continuously flux decline for concentrated 3600 mg/L CaSO₄ solution, the feed solution was heated to 75 °C and then immediate filtered to remove crystals formed in bulk solution during the heating process before the SVMMD test. Comparing with the solution without filtering, the fouling behavior in this case became “two-stage trend” again with an induction time approximately 3 h (Fig. 7). It was further evidence that bulk crystallization, rather than surface crystallization, played the dominate role in the fouling behavior for treating high concentrated supersaturation solution.

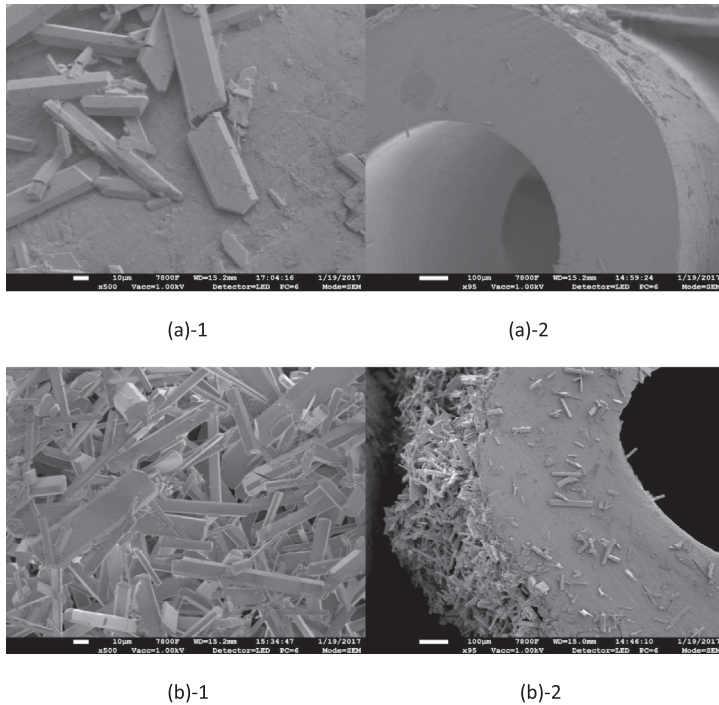


Fig. 6. Effect of initial concentration on the morphology of CaSO₄ fouling layer after experiments. SEM micrographs (a), (b) for initial concentration of 900 mg/L and 3600 mg/L CaSO₄ solution respectively. The outer surface for the left and the cross-section for the right. Experiment conditions: feed temperature 75 °C; vacuum pressure – 85 KPa.

3.2. Membrane scaling mitigation strategies

3.2.1. On-line membrane cleaning

Periodical air backwash was applied as an on-line membrane cleaning strategy to investigate if the fouling and scaling on the membrane could be inhibited. A flow rate of 1.0 L/min compressed air was pushed from the permeate side for 3 min every 2 h in order to reduce salt deposition on the membrane surface or in the membrane pores. The pressure of compressed air was kept at 0.1 MPa.

The result proved that whether periodical air backwash took effect largely depended on crystallization mechanism in concentrating process. If the initial saturation condition of the feed solution made the heterogeneous nucleation on membrane surface play a dominate role, the normalized flux ratio obtained for air backwash was similar to the profile for no air backwash mode, indicating that the generation of air

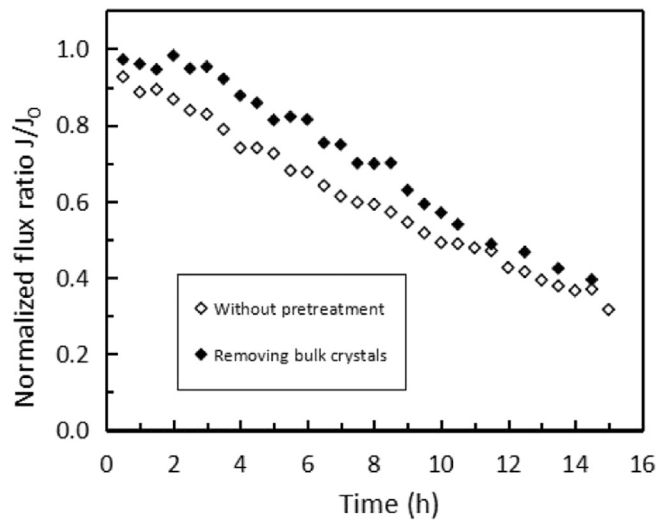


Fig. 7. Normalized flux ratio as a function of operation time for concentrating 3600 mg/L CaSO₄ with and without removing CaSO₄ crystals in bulk solution. Experiment conditions: feed temperature 75 °C; vacuum pressure – 85 KPa.

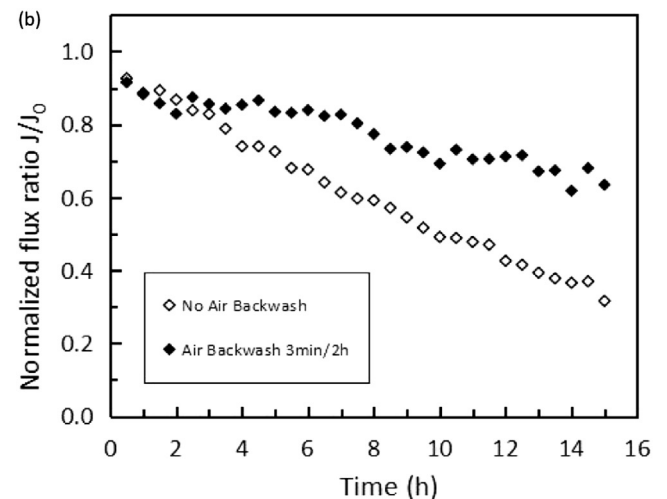
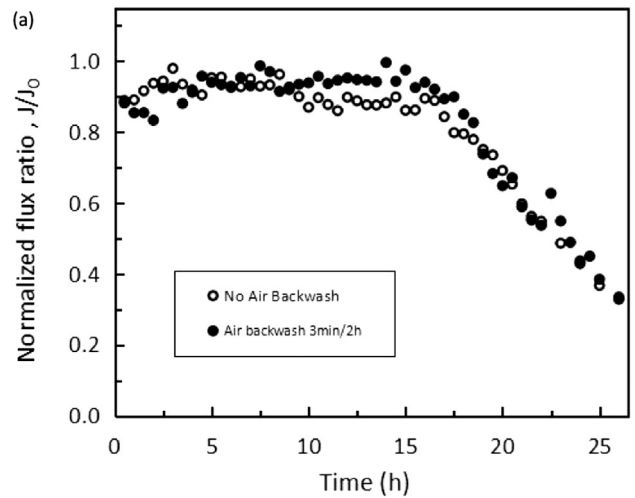


Fig. 8. Normalized flux ratio as a function of operation time for concentrating (a) 1800 mg/L CaSO₄ solution; (b) 3600 mg/L CaSO₄ solution. Experiment conditions: temperature 75 °C; vacuum pressure – 85 KPa.

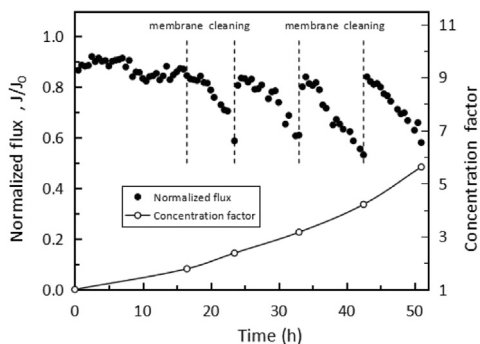


Fig. 9. Normalized flux and concentration factor as a function of operation time for continuously concentrating 1800 mg/L CaSO_4 solution. Experiment conditions: feed temperature 75 °C; vacuum pressure – 85 KPa.

bubbles through backwash had negligible effect on fouling and scaling inhibition (Fig. 8a). Since the fouling layer formed by crystals grew directly on the membrane surface was so strong-adhesion, it was difficult for air bubbles to remove it away although the layer was thin. On the contrary, if homogeneous nucleation in the bulk solution dominated the crystallization process, the deposited layer on the membrane surface became looser and less adhesive, which could be readily removed away from membrane surface by periodically air backwash. Fig. 8b compared fouling rate for concentrating 3600 mg/L CaSO_4 solution with and without the aid of air backwash, it turned out that the fouling rate was reduced by 54% with the help of air backwash, the normalized flux ratio was above 0.6 in 15 h continuously operation.

3.2.2. Off-line membrane cleaning

Membrane flushing is considered as one of the fouling control techniques for MD process. The design of open membrane module made membrane cleaning more convenient. Periodically off-line membrane cleaning with DI water was used prior to the critical point appeared and the experiment was terminated again when the normalized flux reduced to 0.6, off-line water cleaning was repeated three times and the final concentration factor was 5.62.

SEM analysis (Fig. 10) showed that simply water flushing could effectively remove most of the accumulated CaSO_4 crystals from the membrane surface without using any additional chemical agent, with only a small amount of residual crystals and nucleation sites. As it was shown in Fig. 9, the permeate flux after off-line water cleaning could be basically recovered to the initial level of previous cycle. The fouling rate in each cycle was 4.37%/h, 2.60%/h, 3.55%/h, 3.64%/h, respectively. All of them was lower than that was shown in Table 2 with the

fouling rate of 6.63%. Despite all this, the flux attenuation was still inevitable with the increase of concentration factor, which further proved that bulk crystallization was the dominated factor at high saturation degree.

3.3. Membrane fouling model

Proposed by Hermia [33], a dead-end filtration model is widely employed to describe fouling phenomenon in pressure-driven membrane process. Srisurichan [34] applied this cake filtration model to a DCMD process and found that it also corresponded well with MD process when a mixture of humic and calcium feed solution was tested. However, this model represents the flow characteristic for a limited period of operational stage [35] and not suited for all MD process. A previous study of vacuum enhanced DCMD for NaCl and NaCl with CaSO_4 showed that the Hermia's blocking filtration models is not suitable any more due to the rapid fouling occurs in MD once the membrane surface was blocked [36].

In this study, the overall trend of the fouling behavior caused by CaSO_4 ranged from slight fluctuation to a rapid decline could be described by Tansel's first-order kinetic model [35]. In this model, the overall resistance is considered as a combination of time-independent resistance and time-dependent resistance. The simplified model can be described by the following equation.

$$\frac{J}{J_0} = \frac{1}{a + b \cdot e^{t/\tau}} \quad (4)$$

There are three coefficients in this model, coefficient a represents the time-independent resistance and coefficient b represents the time-dependent resistance, coefficient c is the fouling time constant.

All three coefficients were obtained by nonlinear fitting with experimental plots using Matlab. The result of fitting was shown in Fig. 11 and the values of a , b , c under different operation conditions were listed in Table 4.

The analysis of coefficient values showed that the feed temperature mainly affected the value of b . With the increase of feed temperature, the time-dependent resistance increased leading to the critical point appeared earlier. The influence of initial concentration of feed solution on coefficient values was more complicated. When surface crystallization played a dominate role, the value of a was much larger than the value of b , which indicated membrane resistance was a major part and the fouling resistance could be negligible at the beginning. When the process was bulk crystallization controlled (in the case of 3600 mg/L CaSO_4 solution), the value of b was almost equal to the value of a . The existence of fouling resistance in initial condition signifying that bulk crystallization and deposition had already occurred at initial stage and the time dependent stage started right away without exhibiting the

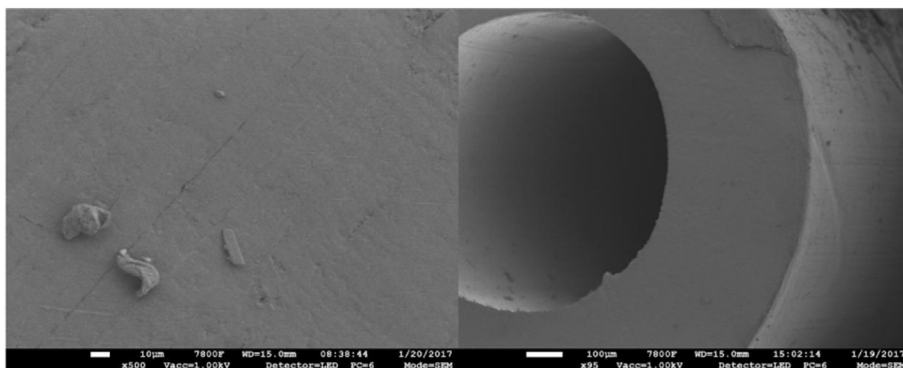


Fig. 10. SEM micrographs of membrane after off-line water cleaning. The outer surface for the left and the cross-section for the right. Experiment conditions: feed temperature of 75 °C; vacuum pressure of – 85 KPa; CaSO_4 solution concentration of 1800 mg/L.

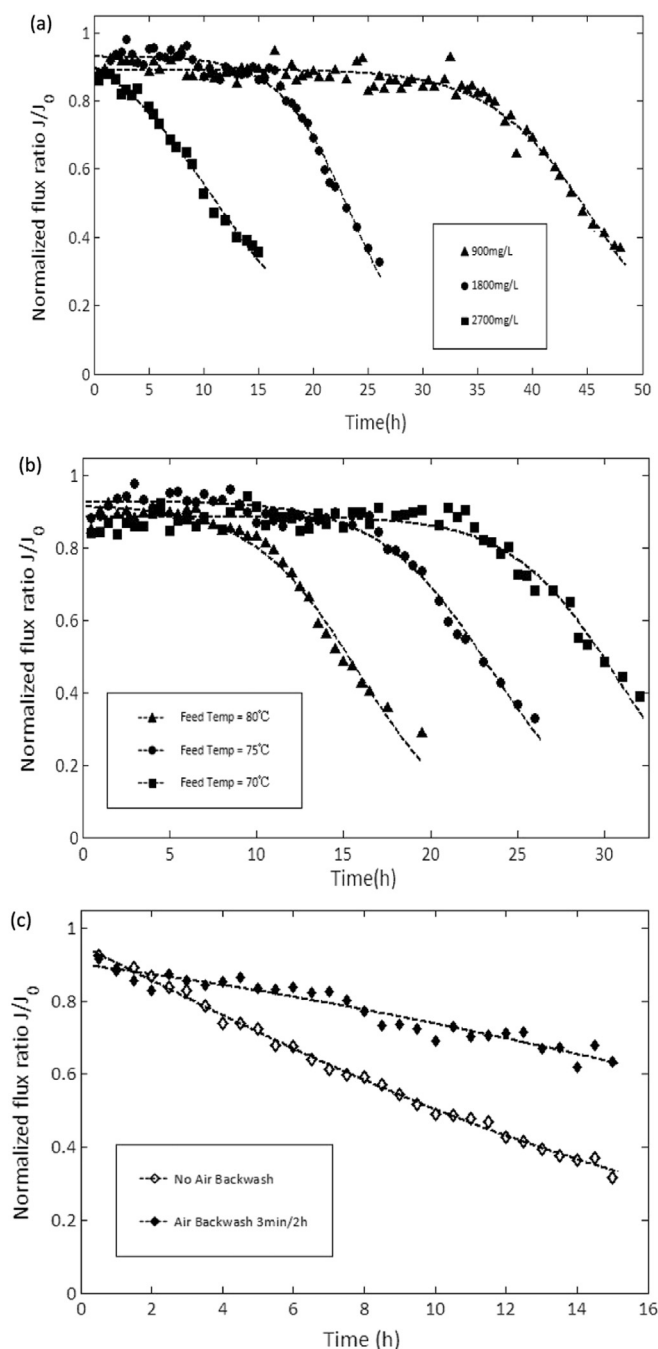


Fig. 11. The result of nonlinear fitting with experimental plots using Matlab. Experiment conditions (a) temperature 75 °C; vacuum pressure – 85 KPa. (b) Feed solution 1800 mg/L CaSO₄; vacuum pressure – 85 KPa. (c) Feed solution 3600 mg/L CaSO₄; temperature 75 °C; vacuum pressure – 85 KPa.

resistance from the membrane. The role of air backwash was mainly for effectively reducing the deposited fouling layer to mitigate membrane fouling rate. It is estimated that nearly 80% of the total time-dependent resistance was the “washable resistance”. The conclusions above were consistent with the fouling behavior of CaSO₄ in Section 3.1.

4. Conclusion

With submerged vacuum membrane distillation (SVMD), stable operation can be achieved for highly concentrated CaSO₄ solution beyond its maximum saturation concentration. But serve fouling was

Table 4
Coefficient values under different operation conditions by nonlinear fitting.

Feed solution	Feed temperature (°C)	a	b	c	R ²
1800 mg/L CaSO ₄ solution	70	1.128	4.317×10^{-5}	3.015	0.9429
	75	1.076	7.278×10^{-4}	3.214	0.9751
	80	1.088	5.738×10^{-3}	3.013	0.9831
900 mg/L CaSO ₄ solution	75	1.122	7.909×10^{-5}	4.775	0.9591
2700 mg/L CaSO ₄ solution		0.9815	0.1298	5.453	0.9888
3600 mg/L CaSO ₄ solution					
No backwash		0.5377	0.5105	9.605	0.996
Air backwash		0.9278	0.1827	11.79	0.9246

observed and flux declined sharply once the feed concentration was higher than a critical level of supersaturation.

There are two mechanisms in CaSO₄ crystal formation process, including membrane surface crystallization and bulk crystallization. Different crystal formation mechanisms lead to different fouling behavior and opposite effects of air bubbles on scaling mitigation.

When surface crystallization played a dominate role (initial feed concentration < 2700 mg/L), the fouling behavior of CaSO₄ presented a typical two-stage trend with the permeate flux remained almost stable in the first stage and followed by a dramatically flux decline in the second stage. The induction time decreased with the increase of feed temperature. Since the fouling layer formed in this case was thin but compact, air-backwash played negligible effect. On the contrary, when bulk crystallization followed by deposition played a more important role (initial feed concentration > 3600 mg/L), the induction time disappeared and permeate flux continued to decrease from the beginning. Although the fouling layer formed was thicker in this case, it became looser and less adhesive, which could be readily removed away from membrane surface by periodically air backwash. The result could be explained by combining the experimental data with an empirical flux decline model.

Acknowledgement

All the authors thank the financial support from Youth Innovation Promotion Association of the Chinese Academy of Sciences (No. 2016171).

References

- [1] M.S. El-Bourawi, et al., A framework for better understanding membrane distillation separation process, *J. Membr. Sci.* 285 (1) (2006) 4–29.
- [2] C.R. Martinetti, A.E. Childress, T.Y. Cath, High recovery of concentrated RO brines using forward osmosis and membrane distillation, *J. Membr. Sci.* 331 (1–2) (2009) 31–39.
- [3] M. Thite, Application of Taguchi method in optimization of desalination by vacuum membrane distillation, *Desalination* 249 (1) (2009) 83–89.
- [4] G. Chen, et al., Optimization of operating conditions for a continuous membrane distillation crystallization process with zero salty water discharge, *J. Membr. Sci.* 450 (2014) 1–11.
- [5] J.P. Mericq, S. Laborie, C. Cabassud, Vacuum membrane distillation of seawater reverse osmosis brines, *Water Res.* 44 (18) (2010) 5260–5273.
- [6] L.D. Tijting, et al., Fouling and its control in membrane distillation—a review, *J. Membr. Sci.* 475 (2015) 215–244.
- [7] M. Gryta, Fouling in direct contact membrane distillation process, *J. Membr. Sci.* 325 (1) (2008) 383–394.
- [8] D.M. Warsinger, et al., Scaling and fouling in membrane distillation for desalination applications: a review, *Desalination* 356 (6) (2015) 294–313.
- [9] H. Fei, et al., Potential for scaling by sparingly soluble salts in crossflow DCMD, *J. Membr. Sci.* 311 (1) (2008) 68–80.
- [10] D.N. Long, T. Cath, A scaling mitigation approach during direct contact membrane distillation, *Sep. Purif. Technol.* 80 (2) (2011) 315–322.
- [11] A. Alkhdhiri, N. Darwish, N. Hilal, Membrane distillation: a comprehensive review, *Desalination* 287 (8) (2012) 2–18.

- [12] L. Francis, et al., Submerged membrane distillation for seawater desalination, *Desalin. Water Treat.* 55 (10) (2014) 1–6.
- [13] S. Meng, et al., Submerged membrane distillation for inland desalination applications, *Desalination* 361 (2015) 72–80.
- [14] H.K. Shon, et al., Physicochemical pretreatment of seawater: fouling reduction and membrane characterization, *Desalination* 238 (1–3) (2009) 10–21.
- [15] J. Wang, et al., Effect of coagulation pretreatment on membrane distillation process for desalination of recirculating cooling water, *Sep. Purif. Technol.* 64 (1) (2008) 108–115.
- [16] A. Razmjou, et al., Superhydrophobic modification of TiO₂ nanocomposite PVDF membranes for applications in membrane distillation, *J. Membr. Sci.* 415–416 (10) (2012) 850–863.
- [17] J. Zhang, et al., Fabrication and characterization of superhydrophobic poly (vinylidene fluoride) membrane for direct contact membrane distillation, *Desalination* 324 (14) (2013) 1–9.
- [18] M. Gryta, Long-term performance of membrane distillation process, *J. Membr. Sci.* 265 (1–2) (2005) 153–159.
- [19] K.J. Hwang, C.S. Chan, K.L. Tung, Effect of backwash on the performance of submerged membrane filtration, *J. Membr. Sci.* 330 (1–2) (2009) 349–356.
- [20] Y. Ye, V. Chen, P. Le-Clech, Evolution of fouling deposition and removal on hollow fibre membrane during filtration with periodical backwash, *Desalination* 283 (12) (2011) 198–205.
- [21] G. Chen, et al., Performance enhancement and scaling control with gas bubbling in direct contact membrane distillation, *Desalination* 308 (1) (2013) 47–55.
- [22] Z. Ding, et al., The use of intermittent gas bubbling to control membrane fouling in concentrating TCM extract by membrane distillation, *J. Membr. Sci.* 372 (1–2) (2011) 172–181.
- [23] E. Drioli, A. Ali, F. Macedonio, Membrane distillation: recent developments and perspectives, *Desalination* 356 (2015) 56–84.
- [24] H. Zhu, et al., Preparation and properties of PTFE hollow fiber membranes for desalination through vacuum membrane distillation, *J. Membr. Sci.* 446 (1) (2013) 145–153.
- [25] J. Jia, G. Kang, Y. Cao, Effect of stretching parameters on structure and properties of polytetrafluoroethylene hollow-fiber membranes, *Chem. Eng. Technol.* 39 (5) (2016) 935–944.
- [26] S. Srisurichan, R. Jiraratananon, A.G. Fane, Humic acid fouling in the membrane distillation process, *Desalination* 174 (1) (2005) 63–72.
- [27] Q. Dan, et al., Study on concentrating primary reverse osmosis retentate by direct contact membrane distillation, *Water Sci. Technol. Water Supply* 247 (1) (2009) 540–550.
- [28] M. Ramezani-pour, M. Sivakumar, An analytical flux decline model for membrane distillation, *Desalination* 345 (345) (2014) 1–12.
- [29] G. Naidu, et al., Application of vacuum membrane distillation for small scale drinking water production, *Desalination* 354 (354) (2014) 53–61.
- [30] T.A. Hoang, H.M. Ang, A.L. Rohl, Effects of temperature on the scaling of calcium sulphate in pipes, *Powder Technol.* 179 (1–2) (2007) 31–37.
- [31] H. Xu, H. Li, D. Wang, Study on CaSO₄ crystallization process and its influential factors, *Ind. Water Treat.* 31 (5) (2011) 67–69.
- [32] H. Julian, et al., Effect of operation parameters on the mass transfer and fouling in submerged vacuum membrane distillation crystallization (VMDC) for inland brine water treatment, *J. Membr. Sci.* 520 (2016) 679–692.
- [33] J. Hermia, Constant pressure blocking filtration law application to powder-law non-Newtonian fluid, *Trans. Inst. Chem. Eng.* 60 (3) (1982) 183–187.
- [34] S. Srisurichan, R. Jiraratananon, A.G. Fane, Mass transfer mechanisms and transport resistances in direct contact membrane distillation process, *J. Membr. Sci.* 277 (1–2) (2006) 186–194.
- [35] B. Tansel, W.Y. Bao, I.N. Tansel, Characterization of fouling kinetics in ultrafiltration systems by resistances in series model, *Desalination* 129 (1) (2000) 7–14.
- [36] G. Naidu, et al., Transport phenomena and fouling in vacuum enhanced direct contact membrane distillation: experimental and modelling, *Sep. Purif. Technol.* 172 (2017) 285–295.